PAPER • OPEN ACCESS

Nanoscale membrane actuator for *in vitro* mechano-stimuli responsive studies of neuronal cell networks on chip

To cite this article: Sijia Xie *et al* 2018 *J. Micromech. Microeng.* **28** 085011

View the article online for updates and enhancements.

Related content

- Microtube array membrane bioreactor promotes neuronal differentiation and orientation
  Sabrina Morelli, Antonella Piscioneri, Simona Salerno et al.

- A microfluidic chip containing multiple 3D nanofibrous scaffolds for culturing human pluripotent stem cells
  Lior Wertheim, Assaf Shapira, Roey J Amir et al.

- The biophysics of neuronal growth
  Kristian Franze and Jochen Guck

IOP ebooks™

Bringing you innovative digital publishing with leading voices to create your essential collection of books in STEM research.

Start exploring the collection - download the first chapter of every title for free.

Nanoscale membrane actuator for *in vitro* mechano-stimuli responsive studies of neuronal cell networks on chip

Sijia Xie[1], J G E Gardeniers[1] and Regina Luttge[2]

[1] Mesoscale Chemical Systems, MESA+ Institute for Nanotechnology, University of Twente, 7500 AE Enschede, Netherlands
[2] Department of Mechanical Engineering, Microsystems Group and ICMS Institute for Complex Molecular Systems, Eindhoven University of Technology, 5612 AZ Eindhoven, Netherlands

E-mail: r.luttge@tue.nl (R Luttge)

Abstract
In order to investigate the hypothesis that dynamic nanoscale stimuli can influence the functional response of the brain, in this paper we describe the development of a membrane actuator chip based on polydimethylsiloxane (PDMS) soft lithography. The chip exerts a local nanoscale mechanical load on an *in vitro* neuronal cell network by microfluidic pneumatic deformation of the membrane. The deformation provides a topographical change in the substrate as an input stimulus for the study of response functions of a neuronal cell network *in vitro*. Calcium ions (Ca^{2+}) imaging within a neuronal cell network grown from dissociated cortical cells of the rat's brain used as a brain model indicates that a neural networks response can be provoked by means of our new method. This actuator chip provides a relatively mild and localised mechanical stimulus by means of a 2% elongation of the membrane's width during the application of a pressure pulse underneath the membrane using a microfluidic channel design. We found an average 50% increase of the intracellular Ca^{2+} flux activity for 2D neuronal cell networks among 4 independent samples cultured on flat membranes. Additionally, we have proven the applicability of the actuator chip for networks on nanogrooved membranes by the observation of Ca^{2+} traces and we also observed the Ca^{2+} waves response upon stimulation in a three dimensional (3D) *in vivo*-like neuronal cell network using Matrigel on flat membranes. Hence, the chip potentially provides a novel technology platform for the *in vitro* modelling of brain tissues with topographically and 3D hydrogel-defined network architectures.

Keywords: nanoscale membrane actuator, mechano-stimuli, neuronal cell networks, calcium imaging

S Supplementary material for this article is available online

(Some figures may appear in colour only in the online journal)

Introduction

The mechanotransduction in neuronal cell networks is a means to communicate between the biochemical and the electrical domain of brain functions [1]. Mechanical properties within the microenvironment of the brain tissue affect various aspects of neuronal processes [2], such as the growth and wiring of the neurites [3, 4], synapse formation [5] and brain circuits activity [6] etc. Modifying biophysical cues due to local mechanical interactions between the extracellular surrounding and the cell adhesion molecules, which can induce intracellular signalling cascades, play an important role in regulating the aforementioned neuronal processes [7].

Introducing Organ on a Chip technology offers an instrumental way to provide such biophysical modification to engineered brain tissues and hence allows to model the brain and better understand its physiology [8–11]. This novel type of a microphysiological brain system provides a platform with considerable advantages, complementary to the high-cost and extremely complicated observations one can collect *in vivo*. One of the major advantages is that a chip-based system enables to precisely tailor the environmental parameters that lead to induce a biological phenomenon of interest [12]. The latter helps neuroscientists and biologists to understand the multimodal effects occurring in neuronal cell networks at the structure level and unravel their cellular and molecular mechanisms being related to the functional level of the brain. Microphysiological devices with various structural and mechanical designs have impressively contributed to this field of biomedical research already [13–17]. Configuring this type of devices based on MEMS technology allows us to control the occurrence of a biological phenomenon temporally and spatially in conjunction with advanced biological, chemical and physical assays that probe these specific physiological processes. The utilisation of soft materials has become popular in developing these devices. Their lower stiffness compared to the conventional rigid substrates used in MEMS technology (e.g. plastics like cyclic olefin copolymer and poly(methyl methacrylate) or actual glass and silicon) improves the mechanical environment for cells particularly for 'soft' biological tissues, like brain, and hence results in morphologies of the cultivated cells that are more comparable with those *in vivo* [18]. Among the extensive elastomer family, polydimethylsiloxane (PDMS) has been a widely used material due to its favourable properties such as high biocompatibility, good optical transparency, and relatively low fabrication costs, and has been applied mostly in fundamental laboratory studies [19]. Moreover, the tuneable stiffness of PDMS realised by varying the ratio between the precursor and the cross-linker components helps to fine-tune substrate stiffness for the many different types of cells under investigation [20]. Furthermore, the elasticity of PDMS makes it easier to introduce various manipulations, such as surface stretching [21, 22] and temporal chamber barrier [23], which helps to realise a microenvironment for an advanced microphysiological system with biomimic functionality on a chip. Hence, it is also our material of choice for the design of the membrane actuator chip platform, which is discussed here.

Therefore, *in vitro* models based on the aforementioned chip technology will contribute to a better understanding of the mechanism of time-space correlated neuro-mechano-responsiveness. The main challenges in studying dynamic neuronal cell network responses upon a locally controlled stimulus on-chip include multi-fold elements. For example, the design of an artificial extracellular environment that is capable of resulting in an *in vivo*-like brain tissue structure, facilitating neuronal cell network formation processes comparable with the architectures of layers and connections found in the brain *in vivo,* is a major challenge. In order to provide such extracellular environment, artificial two dimensional (2D) and three dimensional (3D) scaffolds have been developed to emulate the *in vivo* functions of the extracellular matrix (ECM) of neuronal tissue [24]. Next to mimicking neural tissue organisation by nanotopographies also a technical solution for the culture-on-chip environment must be found that allows to host developing neuronal cell networks in 3D sufficiently long, to accommodate a mature enough phase of neuronal development (>14 d *in vitro*, DIV) which expresses the rich behaviour of neuronal communication and cell to cell interactions (e.g. firing patterns) better reflecting on brain functions *in vivo*. And, essentially, such environment has to be integrated with the capability of producing the distinct mechanical stimuli on a neuronal cell network on-chip according to the various requirements and motivations of the research questions at hand of a neuroscientist.

To explore the effect of localised mechanical stimulation on an *in vitro* neuronal cell network, here, we introduce a novel brain-on-a-chip. The paper discloses the design and fabrication of a PDMS-based membrane actuator chip, which can exert mechanical stimuli at the micro- to nanoscale to an engineered brain tissue cultured in the chip either in 2D or in 3D. As a proof of concept, the responsive activity within the neuronal network of the brain tissue was visualised by fluorescently labelling an important cellular signalling factor: calcium ions [25]. The calcium ions (Ca^{2+}) are involved in regulatory effects of many enzymes and proteins in a cell. The cellular Ca^{2+} activity has already extensively been used as a response indicator for the study of exoteric triggers in neuronal cell networks by using mechanical, chemical or electrical stimulation [26–30]. Cellular calcium signalling proteomes are tissue-specific, producing unique calcium signals that suit a physiological process in the tissue [31]. The transmission of Ca^{2+} has been considered to be an important marker to evaluate neurophysiological processes occurring in a primary cortical cell network [32–34]. Here, Ca^{2+} imaging of the living culture was performed as an approach to observe the intracellular Ca^{2+} activities prior and upon the local stimulus. The Ca^{2+} waves within the neuronal network formed of the dissociated cells of new born rats will give us a first indication towards a better understanding of the intercellular signal communication between different types of cells in combination with immunostaining. We demonstrated the application of the chip with a flat and a nanogrooved membrane and extended the experimental design to a 3D configuration using Matrigel atop of the cell-membrane interface. Our preliminary experimental results on flat membranes showed that the Ca^{2+}
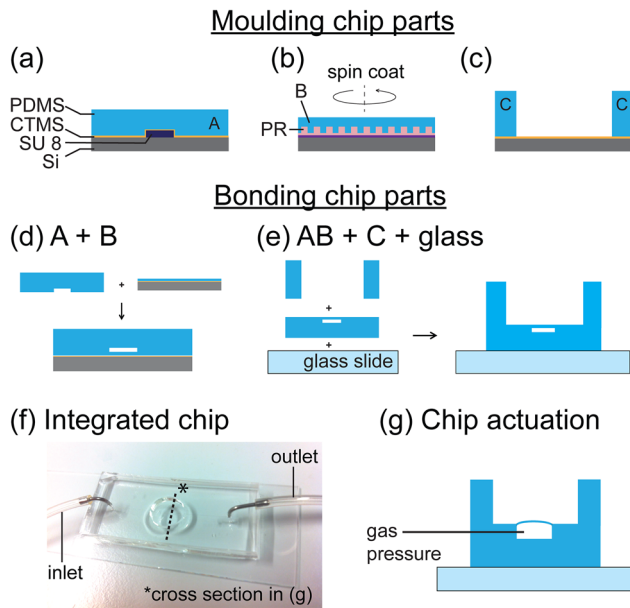
Moulding chip parts

(a)

PDMS
CTMS
SU 8
Si

(b) spin coat

B
PR

(c)

C   C

A

Bonding chip parts

(d) A + B

(e) AB + C + glass

glass slide

(f) Integrated chip

inlet

outlet

*

*cross section in (g)

(g) Chip actuation

gas
pressure

Figure 1. Scheme of the chip fabrication process. (a)–(c) Moulding PDMS chip parts. (d) and (e) Bonding the chip parts. (f) Example of the realised device and (g) a schematic drawing of the mechanism of the chip actuation.

activities respond directly to the mechanical stimulus while in nanogrooved and 3D cultures the response is more complex and will need a more advanced video image analysis. Nevertheless, the results already imply that our membrane actuator chip can be used as a platform to investigate the dynamics of signal transmission in neuronal cell networks.

Methods

Fabricating the actuator chip by PDMS soft-lithography

The actuator chip is composed of three PDMS layers: the underneath channel (A), the flexible membrane (B) and the culture chamber (C), and for greater mechanical stability it is bonded to a microscopy slide. Uncured Sylgard®184 (Dow Corning) was mixed with a certain ratio of the elastomer to the cross-linker for moulding the PDMS layers. In our experiment, 10:1 (elastomer: cross-linker) PDMS was used for fabricating the flexible membrane (layer B). To prevent deformation of the channel width during actuation, the rigidity of the underneath channel (layer A) was strengthened by using a higher cross-linker composition in the uncured PDMS (elastomer: cross-linker = 7:1). The culture chamber (layer C) was prepared with 7:1 PDMS as well. The mixture was hand-stirred with a plastic stick till well blended and then degassed in a vacuum chamber before moulding to remove the air bubbles in the PDMS.

Figure 1 shows the scheme of the main process. Layer A, the underneath channel structure, was moulded by pouring uncured PDMS onto a SU-8 template to achieve a layer thickness of around 1 mm, followed by baking at 80 °C for 30 min (figure 1(a)). The template for moulding the underneath channel (layer A) was fabricated by applying photolithography in SU-8 resist. Details of the fabrication process are

described in section 1 of the supplementary information (S1) (stacks.iop.org/JMM/28/085011/mmedia). The underneath channel template has an average height of 40 μm. Different dimensions of the channel width (10, 25, 50, 100 and 120 μm) were used for the experiment. The SU-8 template was coated with Chlorotrimethylsilane (CTMS) as an anti-stiction layer prior to the PDMS moulding step. Layer B, the membrane, was prepared by spin coating uncured PDMS on a photoresist nanoscaffold template (PR) at 5000 rpm for 5 min, followed by baking at 60 °C for 2 h, resulting in a membrane thickness of 4 μm ($\sigma = 0.2$, N = 6) (figure 1(b)). This PR nanoscaffold was fabricated by Jet and Flash nanoimprint lithography (JIF™), and was directly used as a template for casting PDMS without any surface treatment. Details of the fabrication of the PR nanoscaffold was described in our previous work on neuronal cell alignment [35]. Similarly to the process shown in figure 1(b), a blank silicon wafer was used as substrate for spin coating a PDMS thin membrane with a flat surface. CTMS was coated as an anti-stiction layer on the blank silicon wafer prior to the spin coating step. Layer C, the cell culture well, was prepared by moulding a slab of 2.5 mm × 1.5 mm × 0.6 mm (L × W × H) PDMS on a CTMS coated blank silicon wafer at 80 °C for 30 min (figure 1(c)). A hole was then punched with an 8 mm diameter into the cured PDMS slab (serving as the culturing well) using a round biopsy puncher (BAP Medical, OD 8 mm, 65-MDP8MM 33-37).

To assemble the chip, layer A and B were first bonded as it is displayed in figure 1(d), and the new part A + B was peeled off from the silicon wafer. Inlets and outlets were then punched with a 25-gauge puncher (Syneo Co.). Layer C was bonded to A + B as displayed in figure 1(e). Further, the inlets and outlets were punched through the new part A + B + C with the same puncher. Finally, the stack of combined PDMS parts was bonded to a clean glass slide. The bonding between the different PDMS parts was realised through surface activation by a 1 min air plasma treatment. To avoid the possibility of leakage between parts caused by weak bonding, uncured PDMS was smeared along the side walls of the chip assembly, followed by baking at 80 °C for 1 h. The inlet and outlet were then connected with a stainless-steel tip (angled tip, OD 0.72 mm, Nordson Corporation) and tubing (Tygon R3607, ID 0.51 mm, OD 2.33 mm). The chip was then ready for performing a cell experiment. Figure 1(f) displays a picture of the completed actuator chip and figure 1(g) provides a schematic drawing of its mechanism of actuation using gas flow.

Cell culture

Primary cortical cells dissociated from a new-born rat's brain were used for cell experiments (Mother rat: Wistar Crl:WU from Harlan Sprague Dawley Inc., bred at MIRA institute at University of Twente.). Before seeding the cells, the chip was sterilised by immersion in 70% ethanol (Merck) for 1 h [36, 37]. The chip was then air-dried in a biology safety cabinet and treated with air plasma to enhance the hydrophilicity of the PDMS surface [38], and then coated with polyethyleneimine (PEI; branched, approx. molecular weight 60 000,

50 wt% aq. solution; Acros Organics; CAS: 9002-98-6) to improve cell adhesion. The primary cortical cells were seeded with 3×10^5 cells/chip (approx. 6000 cells mm^{-2}) and cultured with R12H medium according to Romijn *et al* [39] containing 1% Penicillin and Streptomycin, at 37 °C, 5% CO_2 and 95% humidity. In order to provide an *in vivo*-like environment to the culture, an approx. 1 mm thick layer of Matrigel (BD Matrigel™ BasementMembraneMatrix Growth Factor Reduced, 356230, BD Bioscience, diluted to 75% of its original concentration with the R12H medium) was added on top of the 2D cultures at 1 DIV. The detailed protocol of adding the gel layer is described in section 2 of the supplementary information (S2). Culture medium was refreshed every 2 d.

Calcium ions imaging

Cell cultures at 15 ($\pm$3) DIV were loaded with Fluo-4 AM (Fluo-4 Calcium Imaging Kit, F10489, Molecular Probes®) in order to image the activity of the intracellular Ca^{2+} of the entire cell population in the cortical cell networks. The loading process followed the recommended protocol provided by the company. When the culture was loaded with Ca^{2+} indicator, it was placed into the cage incubator of a fluorescence microscope (Nikon confocal A1) for Ca^{2+} imaging and the chip was connected to compressed air flow for actuation. The cage incubator was heated and kept at 37 °C, and air with 5% CO_2 was introduced to the incubator, thus the environment conditions during the live cell imaging experiment were kept as similar as possible to the cell incubator. During imaging, the compressed air was introduced into the chip channel by the control of a pressure regulator (Festo, LRP-1/4-2.5 162834) and a ball valve (Festo), producing deformation in the flexible membrane as a local stimulus to the culture. The intracellular Ca^{2+} activity was recorded with a Nikon fluorescence microscope, with a $10\times$ objective. Images were analysed with Fiji (Image J) software provided by National Institutes of Health [40].

Fluorescent cell staining

Live/dead cell viability assay (Cellstain Double Staining Kit; Sigma Aldrich, 04511) was performed to evaluate the viability of the cortical cell cultures in the actuator chip after stimulation. To identify the cell types in the cortical cell culture, immunostaining was performed when cultures were fixed immediately after a stimulation experiment. Glial fibrillary acidic protein (GFAP) and microtubule-associated protein 2 (MAP2) were stained to identify astrocytes and neurons, respectively. Anti-GFAP antibody (goat; Sigma Aldrich, SAB2500462; 1:200), anti-MAP2 antibody (mouse; Sigma Aldrich, M9942; 1:200) were used as the primary antibodies. Anti-goat IgG (H + L), CF™ 488A (donkey; Sigma Aldrich, SAB4600032; 1:500) and anti-mouse IgG (H + L), highly cross-adsorbed, CF™ 640R antibody (donkey; Sigma Aldrich, SAB4600154; 1:500) were used as the second antibodies.
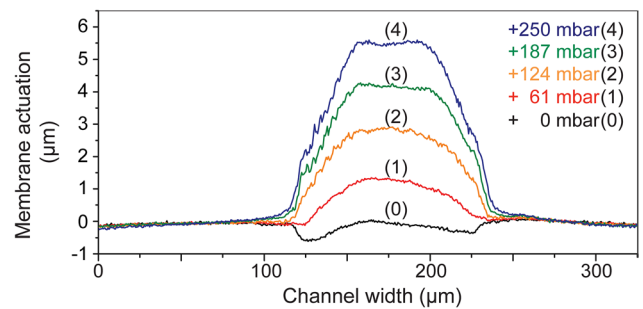

Figure 2. Actuation of the membrane in the chip with gas flow pressure control. The test chip consists of an underneath channel of a width of 120 μm and a membrane with 4 μm thickness. Reproduced with permission from [43]. © CBMS.

Results and discussion

Actuator chip configurations

We realised three types of actuator chip configurations following the protocol described in the Methods section. The protocol consisted of the fabrication and assembly of three layers: underneath channel (layer A), membrane (layer B) and culture well (layer C). The first and second type of actuator chip contained a nanogrooved membrane and a non-patterned membrane for 2D culture, respectively. For a third type of actuator chip configuration we added a layer of diluted Matrigel for *in vivo*-like cell culture allowing to extend the cell culture into the third dimension, based on our previous study [41, 42]. For each configuration repetitive actuator chips were fabricated and utilised in the experimental work. Also, a number of chips with a non-patterned membrane were fabricated only for the characterisation of the chip actuation mechanism.

Each type of the chips was durable for at least 3 weeks under the cell culture conditions applied during our study and were capable of repetitive actuation with/without the cell culture atop. However, for the cell stimulation experiment only one stimulus was applied on each free-standing membrane in order to eliminate any time-delayed effects of the stimulation event on the cells during data recording. Chips for cell stimulation experiments in this work were prepared for one-time use only considering the difficulty in removing and completely cleaning the culture residues from the culturing area without damaging the PDMS surface.

Actuation of the PDMS chip

Compressed air flow was introduced into the chip to produce a deformation in the flexible membrane (figures 1(f) and (g)). The deformation was confirmed with white light interferometry (Polytech MSA-400), and analysed by the Polytec's Topography Measurement System software. White light interferometry results show the deformation of the membrane actuated with different gas flow pressures (figure 2). The deformation in the membrane was estimated by measuring displacement of the membrane and considering an arc for the deformed shape. Subsequently, the change of the arc length due to the displacement was calculated. For example, for a test chip with an underneath channel of a width of 120 μm and a
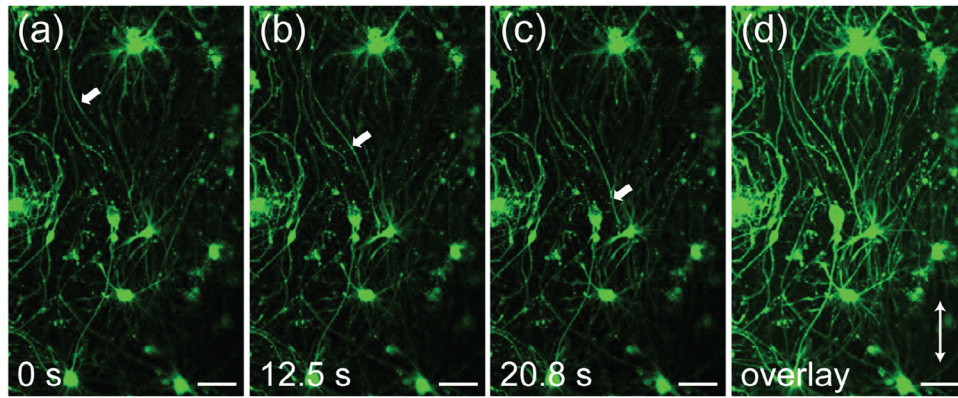
Figure 3. Ca^{2+} transmission in cortical cell network (DIV18) along the cellular outgrowth on a nanopatterned surface. White arrows in (a)–(c) indicate the Ca^{2+} transmission pathway in one outgrowth at time points (a) 0 s, (b) 12.5 s, and (c) 20.8 s as an example. (d) Overlay of the Ca^{2+} fluorescence intensity during 720 s. The white arrow in (d) indicates the direction of the nanogrooves. The original movie is provided as online supplementary information (S4).

membrane actuation of 10 μm high, the membrane is capable to deform approx. 2% of its original width. Hence for the localised deformation within the size of a cell (which is a few micrometres) the membrane would deform at the nanoscale. The details of the calculation and the deformation test are described in section 3 of the supplementary information (S3).

The deformation experiments were carried out on chips without either nanogrooves, PEI coating or cells on top of the membrane as a demonstration. The actual scale of the deformation may change according to the exact stiffness of the membrane, which may be influenced by the nanopatterning of the membrane and loading with the additional chemical molecules and cells during a real cell experiment.

Calcium waves in highly ordered neuronal cell network exploring cortical network response on nanogrooved membranes

It has been demonstrated that the linear nanogrooved pattern ('nanoscaffold' [35]) on the PDMS surface influences the direction of the neuronal outgrowth as well as the organisation of the cortical neuronal cell networks formation in our previous work [35, 44]. Contrastive to the random neuronal network of the primary cortical cells on a non-patterned surface, the neuronal cell network formed on a linear patterned surface is organised with highly ordered cell outgrowths which are aligned with the direction of the line pattern of the nanogrooves. The latter has been revealed by both live/dead staining and fluorescent immunostaining of the cortical cells [35, 44]. Here, Ca^{2+} was used to further visualise the dynamic activities in the live neuronal cell network. As introduced above, the intracellular Ca^{2+} indicator Fluo-4 AM loads on the primary cortical cells without any specificity of the cell type. Therefore, an overall intracellular Ca^{2+} activity was recorded during observation. As a preliminary demonstration, figure 3 displays the Ca^{2+} transmission in a live cortical cell network that formed on a nanoscaffold. An oriented pathway of the Ca^{2+} flux was depicted with the help of the white arrows in figures 3(a)–(c). As stated in our previous work, the directional neuronal outgrowths may present

also a more *in vivo*-like neuronal cell network morphology of brain cortex, where neuron somas are positioned in different cortical layers according to their functions (grey matter), and the neuronal outgrowths are aligned and bundled while the myelinated axons further extend in the white matter, wiring grey matter areas in various brain regions [45]. On the other hand, the highly aligned outgrowths also ease the analysis of tracing the Ca^{2+} flux in the complex primary neuronal cell network along the neuronal outgrowth as depicted in figure 3. If such aligned features of neuronal outgrowth are indeed a predictive model for a functioning brain tissue remains to be elucidated in further studies.

Observation of calcium ion waves upon mechanical stimulation exploring randomly grown cortical cell network on-chip using non-patterned membranes

It is our ultimate goal to study the dynamics of the signal transmission within the neuronal cell network upon mechanical stimulation in an environment more comparable to brain tissue *in vivo*, which is realised here by the linear nanoscaffold. However, for being able to harvest meaningful data, we first investigate the general experimental conditions in more depth. To combine mechanical stimulation experiments with Ca^{2+} wave imaging in 3D *in vivo*-like environments we therefore establish the method using primary cortical culture on-chip with a non-patterned membrane. The latter will form a benchmark for more complex network architectures. As a demonstration of the functioning of the chip, figures 4 and 5 show the Ca^{2+} activities within the entire cortical cell networks, responding to a stimulus with 10 s duration produced by an applied pressure of 200 mbar in the channel, with no specificity for a certain cell type. It is supposed that when a stimulus is applied, the cells that adhered on the free-standing membrane or at the edges of the membrane receive a mechanical stretching stimulus in the order of forces in the nanoscale regime, and hence the cells respond upon this with intracellular Ca^{2+} fluctuation. The signal transduction and transmission among the cells may lead to correlated intracellular Ca^{2+} flux in several neighbouring cells, which can be
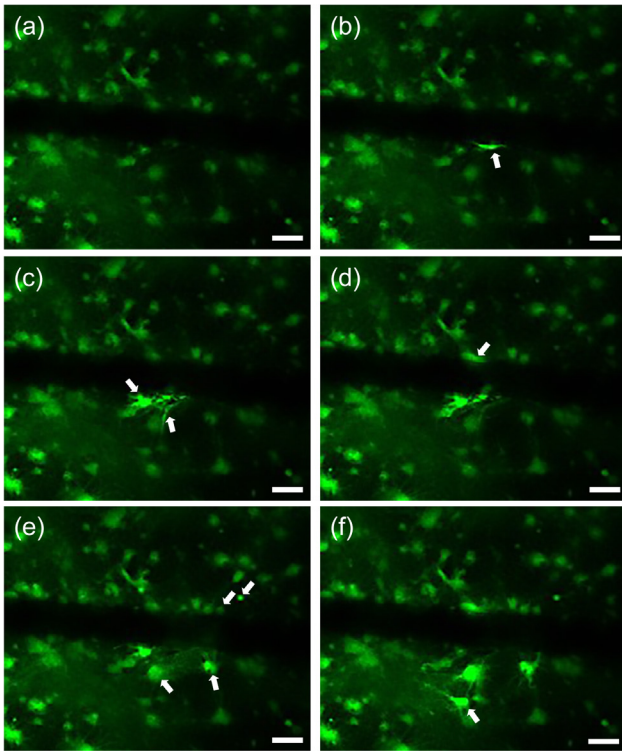
Figure 4. Ca^{2+} waves within a non-patterned *in vivo*-like (cells extend in 3D by means of a layer of gel) cortical cell network activated by the stimulation from the chip with a 50 μm channel width. The black strip area in each figure indicates the location of the underneath microchannel. White arrows indicate the cells that were undergoing a Ca^{2+} flux, revealed by the change of the fluorescence intensity. Time scale (0 s) starts from the introduction of the stimulus: (a) -4 s; (b) 0 s; (c) 16 s; (d) 25 s; (e) 34 s; (f) 70 s. Scale bar: 50 μm. Series of images extracted from video recordings of the observed Ca^{2+} wave, which is provided as online supplementary information (S5).

referred to as intercellular Ca^{2+} waves. Figure 4 displays a series of such Ca^{2+} waves that were caused by the stimulus and spread radially from the channel edges into the surroundings using a non-patterned membrane. The original movie of the Ca^{2+} imaging, of which the series of images depicted in figure 4 were extracted, is provided as online supplementary information (S5).

We assume that the cellular configuration in our design of an *in vivo*-like culture using a layer of Matrigel atop is favourable for a cellular morphology of physiological relevance and it may also allow for better connectivity among the cells in the tested neuronal cell network by its 3D nature as demonstrated by the results presented in figure 4. However, considering the difficulty of imaging and analysing the real-time activity of the multi-layered cells, we continued our thorough quantitative analysis of actuator chip performance with respect to the neuronal cell network dynamics only in the 2D on-chip culture configuration as a proof of principle for the mechano-responsiveness experiments. It is worth noticing that optimisation of this specific culture conditions towards a 3D configuration may yield a more mature neuronal cell network in comparison to 2D for the same time of culturing, which can lead to further advances in the utility of the actuator chip for mechanotransduction studies *in vitro*.

Finally, 2D cultures on the non-patterned chip were used for quantitative analysis of the neuronal response to the mechanical stimulation. Figure 5 shows an example of analysing the related events of Ca^{2+} activities in a culture-on-chip. This Figure presents qualitatively how the Ca^{2+} fluorescence was analysed in our experiment. In figure 5(a) we showed how we selected the regions of interest (ROIs) from the Ca^{2+} imaging videos. And figure 5(b) shows the real-time response of the ROIs, in which the increasing peaks of the fluorescence intensity were considered as the 'Ca^{2+} events' calculated and depicted in figure 6(b). To define ROIs, an area of 700 μm $\times$ 700 μm centred with the middle point of the channel area in each field of view was considered as one sample for the analysis (figure 5(a)). In each of these samples, 15–20 individual cells are identified as regions of interest (ROIs) were analysed for counting the amount of the spikes of the fluorescence intensity (referred to as 'Ca^{2+} events', shown in figure 5(b)). When a stimulus was introduced, an average of 7% increase of the overall fluorescence intensity of the Ca^{2+} compared to the fluorescence intensity prior to the stimuli was observed from N = 4 independent culture-on-chip samples (figure 6(a)). The increase of the total fluorescence intensity implies the activation of the cortical cell network due to the stimulation [46]. In addition, the number of the Ca^{2+} 'events' observed in the ROIs increased around 50%, after a stimulus with 10 s duration produced by a 200 mbar pressure in the channel was carried out in the chip (figures 5(b) and 6(b)), implying that individual cortical cells responded to the mechanical stimulation.

In order to evaluate the potential harm of the mechanical stimulation loaded onto the cells, the stimulated culture was kept incubated with medium for 36 h after the experiment, then it was stained with Calcein-AM/propidium iodide (PI) to show the cell viability. The green staining in figure 7(a) shows a viable cortical cell network near the stimulated region, indicating that the stimulation was strong enough to induce an activated Ca^{2+} flux, without causing fatal harm to the cells. The ROIs for the stimulated region was determined as a 100 $\times$ 1200 μm area aligned with the free standing membrane (i.e. the channel area). The ROIs for the non-stimulated region (the control region) was determined as a 100 $\times$ 1200 μm area which was parallel and of 500 μm distance from the stimulated region. No significant difference of cell viability was observed between the stimulated regions of cells in a culture and the control regions of cells in the same culture, which confirms that the observation of the activities shown in figures 5 and 6 are not a consequence of fatal cell damages or apoptotic events due to the stimulation (figure 7(b)).

A stimulus with 10 s duration and an applied pressure of 200 mbar was used throughout the experiments presented in this paper as a demonstration. It was noticed that the level of the deformation would result in different response patterns of the neuronal cell network. For example, while applying a stimulus with a pressure of 50 mbar, the neuronal cell network samples did not show as obvious Ca^{2+} fluctuation during the same time (3 min after stimulation) as those being stimulated with a pressure of 200 mbar. Hence, further investigation that includes more details of the parameters of the stimulation,
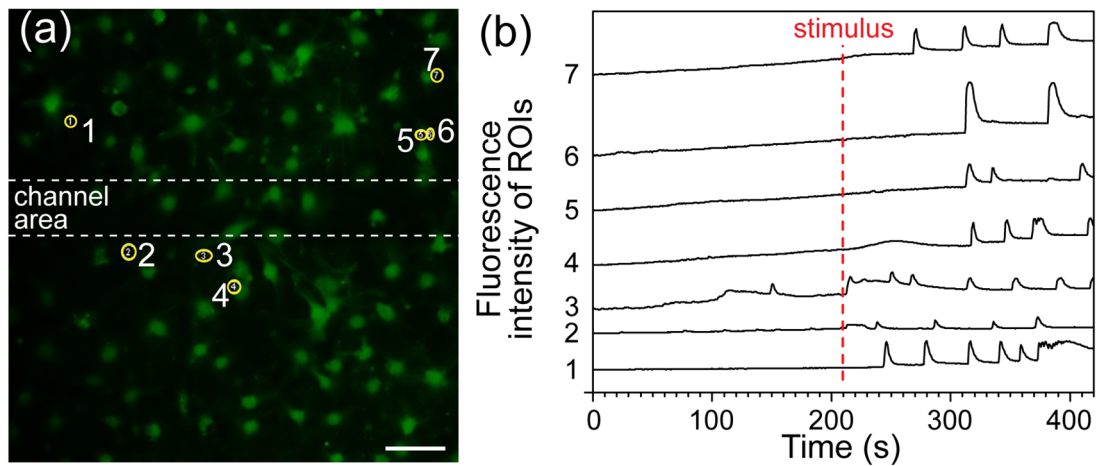
Figure 5. Ca^{2+} imaging of 2D cultured cortical cells in the actuator chip (DIV 14). (a) Primary cortical cells loaded with Ca^{2+} indicator in the chip. The two dashed lines indicate the position of the flexible free-standing membrane and the microchannel underneath. Yellow circles indicate the regions of interest (ROIs) where fluorescence intensity was monitored in (b). Scale bar: 100 μm. (b) Ca^{2+} activities of the selected cells. Numbers correlate with the ROIs in (a). The red dashed line indicates the time point at which a stimulus is introduced. Reproduced with permission from [43]. © CBMS.
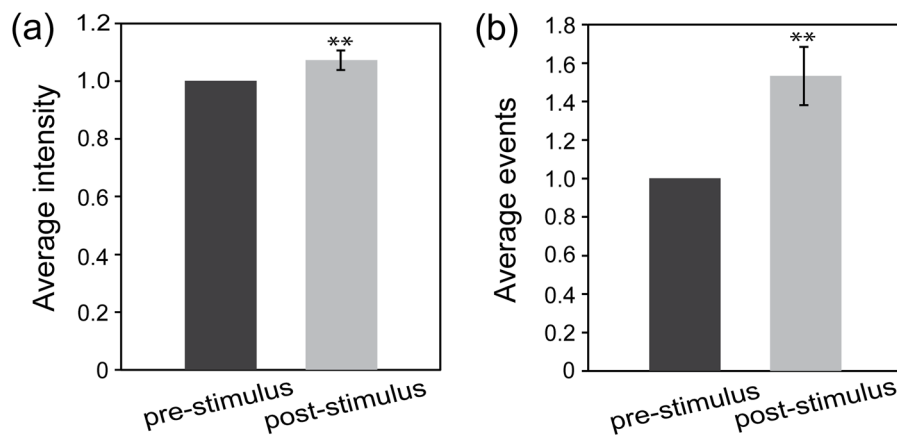

Figure 6. Comparison of the Ca^{2+} fluorescence between before (pre-) and after (post-) a stimulus was applied within the same area and equal time durations. Independent cultures were analysed at DIV 14. (a) The ratio of average fluorescence intensity post-stimulus to pre-stimulus (b) the ratio of the total amount of events of the Ca^{2+} 'events' post-stimulus to pre-stimulus. Definition of the pre- and post- stimulus duration: the 180 s before (pre-) and after (post-) the time point when a stimulus was applied. (N = 4, p < 0.01 in one-way ANOVA analysis with SPSS.) Reproduced with permission from [43]. © CBMS.

such as pressure intensity, the duration of the stimulus, and the width of the freestanding membrane are helpful for understanding the mechanism of the neuro-mechano responsiveness by using this type of actuator chip.

On the other hand, the exposure conditions of the living cell culture are critical technical factors for a successful Ca^{2+} imaging experiment. Experience has shown that excessive exposure time or power of the excitation light (either a mercury lamp or 488 nm laser) causes photobleaching and photodamage in cells in the control samples, which may lead to cell damage or even apoptosis and death. Therefore, optimised illumination is a very important factor in this experiment. For example, if using the mercury lamp as the excitation light source, the interval duration of exposure can be elongated to a few seconds instead of a continuous exposure, since the Ca^{2+} fluctuation take place at a speed of second's to minute's level. In case of the 488 nm laser scanning mode, the parameters such as scan rate and scan area should be coordinated in order to complete scanning an image with a required area in a few seconds. The light intensity in either of the excitation modes should be as low as possible. Moreover, the loading volume and loading time of the Ca^{2+} indicator Fluo-4 AM had to be optimised for various conditions and setups, too. For example, the *in vivo*-like culture within the 3D configuration of the gel needs a longer incubation time compared to the 2D culture, while excessive loading time can also lead to weak activities [47]. In our experiments we loaded the Fluo-4 AM on the cultures with gel for 30 min longer than the 2D cultures. Hence, the gel thickness in future design of the experiment has to be further optimised and reduced to avoid excessive loading times.

Ca^{2+} is an essential intracellular messenger molecule for functioning of almost every cell type in biological organisms. The intracellular Ca^{2+} generates various signals that are involved in a diverse range of cellular processes, such as proliferation, development, fertilisation, learning and memory,
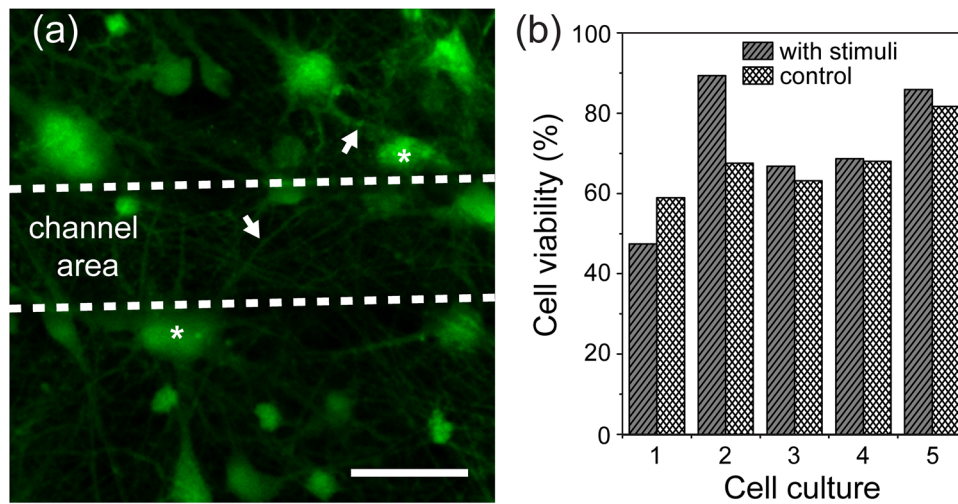
Figure 7. Cell viability of cultures on the chip. (a) A viable cortical cell network (DIV 18) loaded with living cell indicator Calcein-AM. The asterisks indicate the cell somas, and the arrows indicate the cell outgrowths. Scale bar: 50 μm. (b) Cell viability analysis. The cell viability of stimulated ROIs in the culture showed no significant difference with the control ROIs in the same culture ($p > 0.5$ in One-way ANOVA analysis with SPSS).

etc [48]. This ion family also takes part in regulating neuronal processes in the central nervous system, for example, triggering the release of neurotransmitter at synaptic junctions, and contributing to dendritic action potentials through voltage-operated channels [47]. Not only for neurons, the Ca^{2+} activities in glial cells have drawn increasing attention to the neuroscientists. The actively propagated Ca^{2+} wave among astrocytes has led to studies of Ca^{2+} signalling between astrocytes and neurons in a defined co-culture of these two specific types of essential brain cells. It has been reported that astrocytic Ca^{2+} waves modulate neuronal cytosolic Ca^{2+}, e.g. large spike-like increases in neuronal Ca^{2+} levels, suggesting that astrocytes participate directly in neurotransmission [49, 50]. Bidirectional communication between neurons and astrocytes was also demonstrated in brain slices [51, 52]. Besides neurons and astrocytes—the most abundant cell types in the brain tissue, microglia cells are also demonstrated to promote the intracellular Ca^{2+} transmission in astrocytes when sensing an external activation. And conversely, activated astrocytes influence the microglial activity via calcium waves [53–56]. The global characterisation of the cortical cell network Ca^{2+} dynamics [57] reveals a part of the big 'jigsaw puzzle' of the brain's functioning and its response at the cellular level to the changes of environmental conditions. In our experiments, the astrocytes (figure 8(b)) and neurons (figure 8(c)) were each immunostained with specific markers to help collect more detailed information from the cortical cells that were involved in Ca^{2+} wave activity. The immunostaining results were compared to the Ca^{2+} imaging results (figure 8(a)) at the same field of view. The matching results in figures 8(d) and (e) show that some of the transient signal events came from the area where MAP2 positive cells were located. The identification of neurons in the cortical cell culture supports the hypothesis that the stimuli activates intracellular neuronal activities and potentially affects the neurotransmission within neural networks. As the Ca^{2+} activities are closely

involved in neurotransmission, they can be an indicator for neuroelectrophysiological activity, too [58–60]. In combination with extracellular electrical signal read-out by this optical means of readout, the actuator chip can already serve as a platform for *in vitro* brain disease models and help to elucidate dysfunctional network response, such as in epilepsy [61, 62].

Cortical neurites can be hundreds of micrometres long, and the Ca^{2+} loading was usually not effective enough to make them visible and identifiable within a complex cortical cell network. Hence, at this stage it is not clear whether a stimulus directly activated a neuron at a contacted neurite, or whether the trigger was transmitted among the cells of the network through intercellular signal cross-talk. More detailed studies should proceed to better understand the transmitting mechanisms among different cell types in the cortical cell networks, for example, using gene transfected neurons and Sulforhodamine-101 marked astrocytes [63] in a laboratory dedicated to neuroscience. The latter will help to identify the cell types during calcium imaging *in situ*, which would be more precise compared to the methods by post-experimental immunostaining, since the cells might migrate a few micrometres per minute during the time of experiments.

As discussed above, the highly ordered cell network as depicted in figure 3 could serve as a model for studying the intercellular Ca^{2+} transmission. However, whether and how the response pattern of the cortical network would change with the influence of the nanoscaffold requires further investigation. Would the organised cortical network provide a more efficient signal transmission among the neurons? Or would it inhibit the efficiency of cell–cell communication because of the confinement of the outgrowth contact points among cells due to the directionally stratified network formation? Further dynamic experiments and analysis on the understanding of pathways of the Ca^{2+} activities need to be carried out to answer these questions.
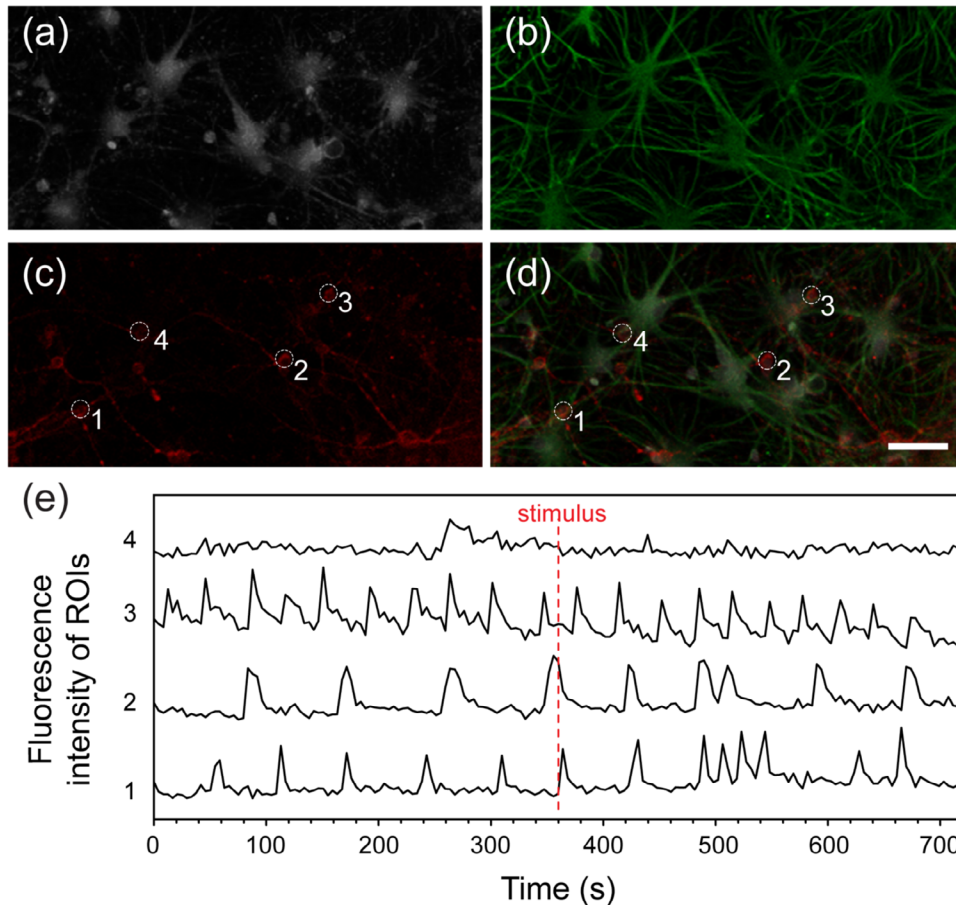
Figure 8. Cell identification combining the immunostaining and Ca^{2+} imaging results in a 2D culture. (a) Cortical cells loaded with Ca^{2+} indicator. (b) Staining of astrocyte's GFAP. (c) Staining of neuron's MAP2. (d) Overlay of (a)–(c). The dashed circles indicate the ROIs for Ca^{2+} activity analysis. Scale bar: 50 μm. (e) Ca^{2+} activities of several neurons as examples. The numbers are correlated with the ROIs in (d). The red dashed line indicates the time point when a stimulus was introduced. The upper edge of this field of view was next to a 50 μm wide channel.

Control network functional behaviour by environmental design

The freedom of design of the actuator chip provides a platform for a relatively 'mild' and localised mechanical stimulation through nanoscale stretching of the membrane, which can be another approach to a novel *in vitro* brain stimulating model, complementary to the conventional stimuli such as harsh strain [64], poking, pressing, or frequency treatment [65, 66]. The possibility to manipulate the stimulation, as well as to topographically functionalise the surface of the integrated flexible membrane in the chip could further benefit the study of mechanotransduction in neuronal cellular networks. The three particular configurations of the chip in this study demonstrate the general functionality of the chip layout using air pressure deformed membranes in the experimental design and the importance of nanoscale cues in the environment to control specific network behaviour. An integrated nanogrooved scaffold on the freestanding membrane provides structural guidance and stratifies the neuronal cell network formation on-chip, which can be an approach to an *in vitro* model of the brain that provides a tissue structure (for example, the white matter, which contains parallel bundles of axons) in the cell culture experiment which is more comparable to the

in vivo architecture of the brain. A supplementary gel layer also improves the cell culture conditions and provides a step forward to *in vivo*-like cell culture environments. Further attempts towards combinations of a 3D culture and a nanoscaffold on the substrate or advanced structurally designed 3D scaffold may be an efficient strategy to realise *in vivo*-like neuronal cell networks on-chip. This type of a functionalised actuator chip can be a practical tool for mechano-stimuli-responsiveness studies of the neuronal cell network *in vitro*.

Conclusions

In this paper, the concept of exerting nanoscale mechanical stimulation to the primary cortical neuronal cells through an elastic actuator chip was tested. The PDMS chip was demonstrated to be capable to produce stimulation through localised mechanical stretching integrated with the cell culture chamber. Cellular calcium ion activity changes were also successfully observed, which implies that cortical cells in the network respond to the stimulation. Results show that the intracellular Ca^{2+} influx responds to a stimulus within seconds and may lead to intercellular Ca^{2+} waves. On average, the frequency of the intracellular Ca^{2+} fluctuation activity increased 50% after

a stimulus was applied. Particularly, an increase of the neuron intracellular Ca^{2+} influx was observed. Hence we believe that this actuator chip can provide a valuable *in vitro* platform to better understand the neuronal cell networks dynamics of the brain either in the healthy or the diseased state.

Acknowledgments

ORCID iDs

Sijia Xie https://orcid.org/0000-0002-9588-1757
J G E Gardeniers https://orcid.org/0000-0003-0581-2668
Regina Luttge https://orcid.org/0000-0002-8486-5866

References

[1] Bystron I, Blakemore C and Rakic P 2008 *Nat. Rev. Neurosci.* **9** 110–22
[2] Tyler W J 2012 *Nat. Rev. Neurosci.* **13** 867–78
[3] Franze K *et al* 2009 *Biophys. J.* **97** 1883–90
[4] Wieringa P, Tonazzini I, Micera S and Cecchini M 2012 *Nanotechnology* **23** 275102
[5] Chavis P and Westbrook G 2001 *Nature* **411** 317–21
[6] Tufail Y, Yoshuhiro A, Pati S, Li M M and Tyler W J 2011 *Nat. Protocols* **6** 1453–70
[7] Sheng L, Leshchyns'ka I and Sytnyk V 2013 *Cell Commun. Signal.* **11** 94
[8] Pamies D, Hartung T and Hogberg H T 2014 *Exp. Biol. Med.* **239** 1096–107
[9] Taylor A M, Blurton-Jones M, Rhee S W, Cribbs D H, Cotman C W and Jeon N L 2005 *Nat. Methods* **2** 599–605
[10] Park J, Koito H, Li J and Han A 2012 *Lab Chip* **12** 3296–304
[11] Soe A K, Nahavandi S and Khoshmanesh K 2012 *Biosens. Bioelectron.* **35** 1–13
[12] Moraes C, Mehta G, Lesher-Perez S C and Takayama S 2011 *Ann. Biomed. Eng.* **40** 1211–27
[13] Huh D, Hamilton G A and Ingber D E 2011 *Trends Cell Biol.* **21** 745–54
[14] Huh D, Kim H J, Fraser J P, Shea D E, Khan M, Bahinski A, Hamilton G A and Ingber D E 2013 *Nat. Protocols* **8** 2135–57
[15] Bhatia S N and Ingber D E 2014 *Nat. Biotechnol.* **32** 760–72
[16] Jiang B, Zheng W, Zhang W and Jiang X 2014 *Sci. China Chem.* **57** 356–64
[17] van der Meer A D and van den Berg A 2012 *Integrat. Biol.* **4** 461–70
[18] Guo W H, Frey M T, Burnham N A and Wang Y L 2006 *Biophys. J.* **90** 2213–20
[19] Anderson J R, Chiu D T, Wu H, Schueller O J and Whitesides G M 2000 *Electrophoresis* **21** 27–40
[20] Brown X Q, Ookawa K and Wong J Y 2005 *Biomaterials* **26** 3123–9
[21] Huh D, Matthews B D, Mammoto A, Montoya-Zavala M, Hsin H Y and Ingber D E 2010 *Science* **328** 1662–8

[22] Douville N J, Zamankhan P, Tung Y-C, Li R, Vaughan B L, Tai C-F, White J, Christensen P J, Grotberg J B and Takayama S 2011 *Lab Chip* **11** 609–19
[23] Shi M, Majumda D, Gao Y, Brewer B M, Goodwin C R, Mclean J A, Li D and Webb D J 2013 *Lab Chip* **13** 3008–12
[24] Dvir T, Timko B P, Kohane D S and Langer R 2011 *Nat. Nanotechnol.* **6** 13–22
[25] Clapham D E 2007 *Cell* **131** 1047–58
[26] Demer L L, Wortham C M, Dirksen E R and Sanderson M J 1993 *Am. J. Physiol. Heart. Circ. Physiol.* **264** H2094–102
[27] Brown T D 2000 *J. Biomech.* **33** 3–14
[28] Bootman M D, Lipp P and Berridge M J 2011 *J. Cell Sci.* **114** 2213–22
[29] Ito S, Suki B, Kume H, Numaguchi Y, Ishii M, Iwaki M, Kondo M, Naruse K, Hasegawa Y and Sokabe M 2010 *Am. J. Respir. Cell Mol. Biol.* **43** 26–34
[30] Jones T J and Nauli S M 2012 *Calcium Signalling* **740** 1001–15
[31] Berridge M J, Bootman M D and Roderick H L 2003 *N. Rev. Mol. Cell Biol.* **4** 517–29
[32] Rochefort N L, Jia H and Konnerth A 2008 *Trends Mol. Med.* **14** 389–99
[33] Grienberger C and Konnerth A 2012 *Neuron* **73** 862–85
[34] Wang X, Takano T and Nedergaard M 2009 *Dynamic Brain Imaging: Multi-Modal Methods and In Vivo Applications* vol 489 (New York: Humana Press) pp 93–109
[35] Xie S and Luttge R 2014 *Microelectron. Eng.* **124** 30–6
[36] Ahmed M, Punshon G, Darbyshire A and Seifalian A M 2013 *J. Biomed. Mater. Res.* B **101** 1182–90
[37] Di Carlo D, Wua L Y and Lee L P 2006 *Lab Chip* **6** 1445–9
[38] Fuard D, Tzvetkova-Chevolleau T, Decossas S, Tracqui P and Schiavone P 2008 *Microelectron. Eng.* **85** 1289–93
[39] Romijn H J, van Huizen F and Wolters P S 1984 *Neurosci. Biobeh. Rev.* **8** 301–34
[40] The FIJI Software (https://fiji.sc/)
[41] Frimat J M S, Xie S, Bastiaens A, Schurink B, Wolbers F, den Toonder J and Luttge R 2015 *J. Vac. Sci. Technol.* B **31** 06F902
[42] Xie S 2016 *PhD Thesis* University of Twente ch 5
[43] Xie S, Gardeniers J G E and Luttge R 2016 *Proc. of the 20th Int. Conf. on Miniaturized Systems for Chemistry and Life Sciences (μTAS) (Dublin, Ireland, 9–13 October 2016)*
[44] Xie S, Schurink B, Wolbers F, Hassink G and Luttge R 2014 *J. Vac. Sci. Technol.* B **32** 06FD03
[45] Bear M F, Connors B W and Paradiso M A 2007 *Neuroscience: Exploring the Brain* 3rd edn (Baltimore, MD: Williams & Wilkins) ch 7
[46] Möller T 2002 *Glia* **40** 184–94
[47] Bootman M D, Rietdorf K, Collins T, Walker S and Sanderson M 2013 *Cold Spring Harb. Protoc.* **2013** 83–99
[48] Berridge M J, Lipp P and Bootman M D 2000 *Nat. Rev. Mol. Cell Biol.* **1** 11–21
[49] Berridge M J 1998 *Neuron* **21** 13–26
[50] Nedergaard M 1994 *Science* **263** 1768–71
[51] Parpura V, Basarsky T A, Liu F, Jeftinija K, Jeftinija S and Haydon P G 1994 *Nature* **369** 744–7
[52] Pasti L, Volterra A, Pozzan T and Carmignoto G 1997 *J. Neurosci.* **17** 7817–30
[53] Pascual O, Casper K B, Kubera C, Zhang J, Revilla-Sanchez R, Sul J-Y, Takano H, Moss S J, McCarthy K and Haydon P G 2005 *Science* **310** 113–6
[54] Liu W, Tang Y and Feng J 2011 *Life Sci.* **89** 141–6
[55] Davalos D, Grutzendler J, Yang G, Kim J V, Zuo Y, Jung S, Littman D R, Dustin M L and Gan W-B 2005 *Nat. Neurosci.* **8** 752–8
[56] Verderio C and Matteoli M 2001 *J. Immunol.* **166** 6383–91
[57] Cossart R, Ikegaya Y and Yuste R 2005 *Cell Calcium* **37** 451–7

[58] Mao B Q, Hamzei-Sichani F, Aronov D, Froemke R C and Yuste R 2001 *Neuron* **32** 883–98

[59] Stosiek C, Garaschuk O, Holthoff K and Konnerth A 2003 *Proc. Natl Acad. Sci.* **100** 7319–24

[60] Ikegaya Y, Aaron G, Cossart R, Aronov D, Lampl I, Ferster D and Yuste R 2004 *Science* **304** 559–64

[61] Cain S M and Snutch T P 2010 *Epilepsia* **51** 11

[62] Weiergräber M, Stephani U and Köhling R 2010 *Brain Res. Rev.* **62** 245–71

[63] Hirase H, Qian L, Barthó P and Buzsáki G 2004 *PLoS Biol.* **2** e96

[64] Geddes-Klein D M, Schiffman K B and Meaney D F 2006 *J. Neurotrauma.* **23** 193–204

[65] Suzuki H, Kerr R, Bianchi L, Frøkjaer-Jensen C, Slone D, Xue J, Gerstbrein B, Driscoll M and Schafer W R 2003 *Neuron* **39** 1005–17

[66] Gurkoff G G, Shahlaie K and Lyeth B G 2012 *Epilepsia* **53** 53–60